NTNU – Trondheim
Norwegian University of
Science and Technology

Simple Well-Model Based on Basic Physical Principles

Ane Cecilie Duus

Chemical Engineering and Biotechnology
Submission date: June 2013
Supervisor: Sigurd Skogestad, IKP
Co-supervisor: Chriss Grimholt, IKP

Norwegian University of Science and Technology
Department of Chemical Engineering

1 Abstract

To reduce loss, real-time optimization (RTO) is today used in most petroleum industry. Minimizing loss is achieved by avoiding over- or underutilization of the production system, and keeping the process as close to the capacity constraints as possible. The dynamic nature of the petroleum extraction makes the process conditions change rapidly. An example is the fluctuating feed and compositions from the wells, which causes a "drift" in the gas-oil ratio(GOR). The changing process conditions will affect the optimal set-points, thus, a frequent re-optimization is necessary to keep the operation close to the optimum. A challenge is that a frequent re-optimization requires updated measurements and a very good model for both process and disturbances. This can be difficult to retrieve.

Self-optimizing control is an alternative to circumvent the whole process of continuous re-optimization. The concept of this method is to control variables which, when held at a constant set-point, can keep the process close to the optimum and this way keep the loss at an acceptable level.

The scope of this thesis is to develop a simple MATLAB-model of a petroleum well by using basic physical principles. The model can later be used locate good control variables (CV's) for self-optimizing control. To verify the flow and pressure conditions in our model, a similar model is made in OLGA, which is leading simulation software in the field of simulating multiphase transport through pipelines.

Prior to making the model, a test is conducted where we find that the well head pressure is a potential self-optimizing variable in our system. By simulations in OLGA we find that the the flow from the reservoir into the well is a linear function of bottom hole pressure, and therefore that Darcy's law can give a good estimation of these relations. OLGA simulations also verify that

the compressibility equation of state gives a good estimate for the pressure profile through the pipe. For the density profile, however, this estimation is slightly more inaccurate. Finally, two different approaches for valve modelling is studied; the *Valve Equation Approach* and the *Bernoulli Approach*. Here we find that the valve equation is best suited for our case.

The model works best for the or the purpose of obtaining information on trends and approximate pressure-values at different as a function of valve opening. However, this is a *very* simplified model, which is also partly adapted to dataseries obtained from OLGA, and should therefore be improved at several areas and tested before used for other purposes.

2 Acknowledgements

I would like to thank the following people for their contributions to this project:

– Sigurd Skogestad, for the project assignment and guidance throughout the project.

– Chirss Grimholt, for project assignment, guidance and help along the way.

– Jan Olav Alstveit, for motivation and support.

– Hvar Lee Loftheim, Tone Alice Tveit, Annette Stokkeland, and ÃŸystein Duus for carefully prof-reading of the thesis.

Contents

List of Tables

List of Figures

3 Introduction

Today, real-time optimization(RTO) is used in most petroleum industry, with the objective to minimize loss. This is achieved by avoiding over- or under-utilization of the production system, and keeping the process as close to the capacity constraints as possible. Normally, this optimization is made once a day, under the assumption of constant well-conditions during this period. In reality, these conditions will change. An example is the fluctuating feed and compositions from the wells, which causes a "drift" in the gas-oil ratio(GOR). Changing process conditions will also change the optimal values for the control variables used to optimize the process, and will lead to sub-optimal operation between each optimization. To minimize the loss, a frequent re-optimization is necessary.

A challenge is that a frequent re-optimization requires an updated model with updated data, which as Foss(2012) points out, can be difficult to retrieve. This is one of the reasons to the growing interest in using results from process control theory to increase the recovery in petroleum reservoirs. In the paper by Jansen, Bosgra and van den Hof(2008), the potential of using control theory to develop model-based control of multiphase ïňĆow in petroleum reservoirs is discussed.

Self-optimizing control is an alternative, where we can circumvent the whole process of continuous re-optimization. The concept of this method is to control variables which, when held at a constant set-point, can keep the process close to the optimum and this way keep the loss at an acceptable level. For these variables, the optimal point also changes minimally due to the effect of disturbances. This is discussed in the paper by Skogestad(1999).

The scope of this thesis is to develop a simple MATLAB-model of a petroleum well by using basic physical principles. The model can later be used to iden-

tify good control variables (CV's) for self-optimizing control. To verify the flow and pressure conditions in our model, a similar model is made in OLGA, which is leading simulation software in the field of simulating multiphase transport through pipelines. The model will describe pressure and flow relations from the bottom hole, where the petroleum mixture flows in from the reservoir, to the valve at wellhead. The model can be divided in three parts, which are based on different models and theory. In the finished model, the parts are connected together and made a function of the valve opening, as this often is the only variable that can be manually manipulated in a well.

A requirement for a self-optimizing variable is that it should be sensitive to input changes. Prior to making the model, we therefore test if we can detect changes in the GOR by measuring the wellhead pressure. The results shows that there is a detectable change in wellhead pressure, as the reservoir gas ratio is increased by 10%. We find that the well head pressure is a potential self-optimizing variable in our system, and that it therefore is interesting to proceed developing the model.

In this thesis, we first present the background and motivation for developing the model. Section 1 presents this, together with the results from testing the wellhead pressure's potential as a self-optimizing variable. We find that the pressure is affected by a shift in the GOR, and therefore can be a candidate as a self-optimizing variable for the system. Following this, in section 2, a description and specifications of the OLGA model is given. Here tables and a figure of the model can be found. The three following sections, will describe each part of the MATLAB-model. Theory, results and discussion of the inflow-model, pipeflow-model and valve-model will be presented in section 3,4 and 5 respectively.Finally, are some concluding remarks and an overview of the literature that is used in this thesis.

Part I

Motivation

4 Background and Motivation

A petroleum field can have more than hundred production wells connected to the process platform by manifolds and pipelines. An illustration of the Troll West rim is presented in Figure 1, where a number of wells produce a mixture of gas, water and oil which is collected in manifolds at the seabed and transported in larger pipelines to the separation facilities at the production platform at sea level.

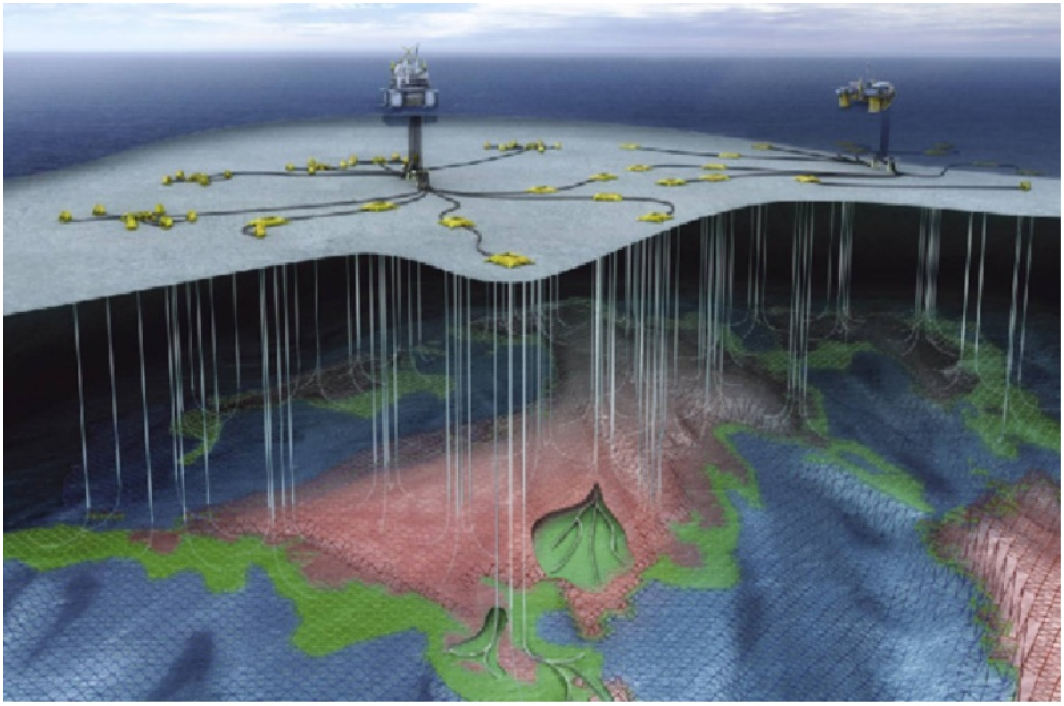

Figure 1: An illustration of the Troll West rim. Gunnerud and Foss (2009).

The wells can be at different depths in the reservoir, and due to heterogeneity in the reservoir formation, the wells will produce different petroleum mixtures of different compositions. As the separation process is expensive, and the capacity of water and gas in the separation facilities are limited, the production structure is optimized so that the wells that produce the highest oil composition will produce at the highest production rate. Optimization is normally made once a day, with the assumption of constant well-conditions during this period. The challenge is that, in a realistic case, these conditions will change. This means that the operation will run suboptimally until the process is re-optimized.

In petroleum production a well-known phenomena is the shift in the gas-oil ratio(GOR), that occurs after the well has produced for some time. During production, the pressure near the well decreases, and causes the well to produce a higher amount of gas. At this point it can be beneficial to re-optimize the production structure, and gain a higher production rate from wells with a lower GOR. This will maximize the total oil production, and minimize the total production of water and gas.

4.1 Optimization Theory

As explained above, the well performance will decrease during production. A change in the process conditions implies that the values for optimal well pressures also will change as illustrated in Figure 2.

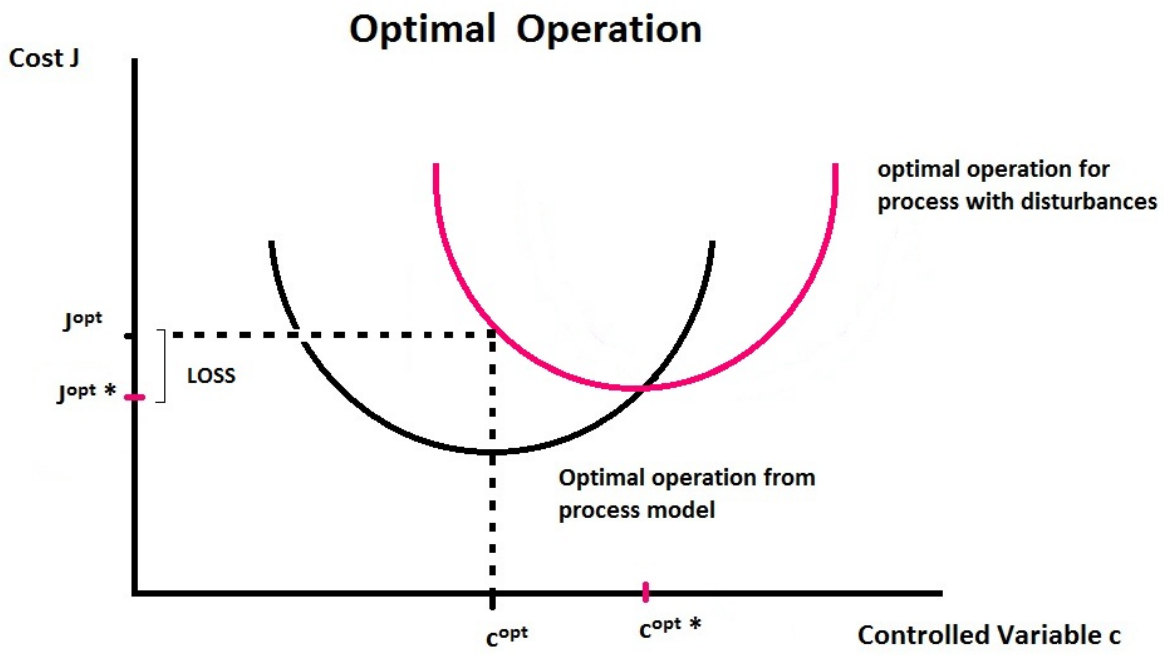

Figure 2: The process disturbence's effect on optimal operating conditions.

Figure 2 illustrates how the optimal operational conditions shift under impact of disturbances. Keeping the controlled variables at the their "old" optimal values will make the process run sub-optimal and therefore lead to a loss. To keep the process at optimal operation, a frequent re-optimizing of the system is needed. This is costly, time consuming, and requires a very good model for both process and disturbances.

To avoid re-optimizing it would be beneficial to control variables where, when held at a constant set-point, can keep the process close to optimum and this way keep the loss at an acceptable level. Variables with this property are termed *self optimizing variables*. The concept of self-optimizing variables will be elaborated on it the next section.

4.1.1 Self-Optimizing Control

The idea of self-optimizing control is, as mentioned in the previous section, to control certain variables that makes it possible to circumvent the whole process of continuous re-optimization. We want to control variables which, when held at a constant set-point, can keep the process close to the optimum and this way keep the loss at an acceptable level. This involves that the optimal set-point for these variables changes minimally due to the effect of disturbances. The procedure of finding self-optimizing variables requires a process model and a cost function to be minimized.

As stated in the paper by Skogestad(2000), a self-optimizing variable should satisfy the following requirements:

1. Its optimal value is insensitive to disturbances i.e $\frac{\triangle c_{opt}}{\triangle d} = small$
2. Its value should be sensitive to input changes i.e $\frac{\triangle c}{\triangle u} = large$
3. It should be easy to measure and control

There is a handful of methods for identifying self optimizing structures. Examples are: *"Null space method"* and *"Exact local method"*, but these methods will not be elaborated on in this paper.

4.2 Wellhead Pressure as Self-Optimizing Variable

It is interesting to look at the potential for the wellhead pressure to be a self-optimizing variable for our system. As stated in section 4.1.1, a self-optimizing variable should be sensitive to input changes. In our system, this means that the the wellhead pressure should be sensitive to a change in the GOR. Prior to making the model, there is therefore first made a test to see if there is any relationship between the wellhead pressure and the GOR in the reservoir.

4.2.1 Result of Sensitivity Test

The wellhead pressure is first measured for valve openings between 0.01 and 1. Then the reservoir gas fraction is increased by 10%, and the same measurements of the wellhead pressure are conducted. The results are plotted and presented in Figure 3.

From Figure 3 we see that the wellhead pressure is affected by the shift in GOR. The pressure difference at valve openings above 0.1 is approximately

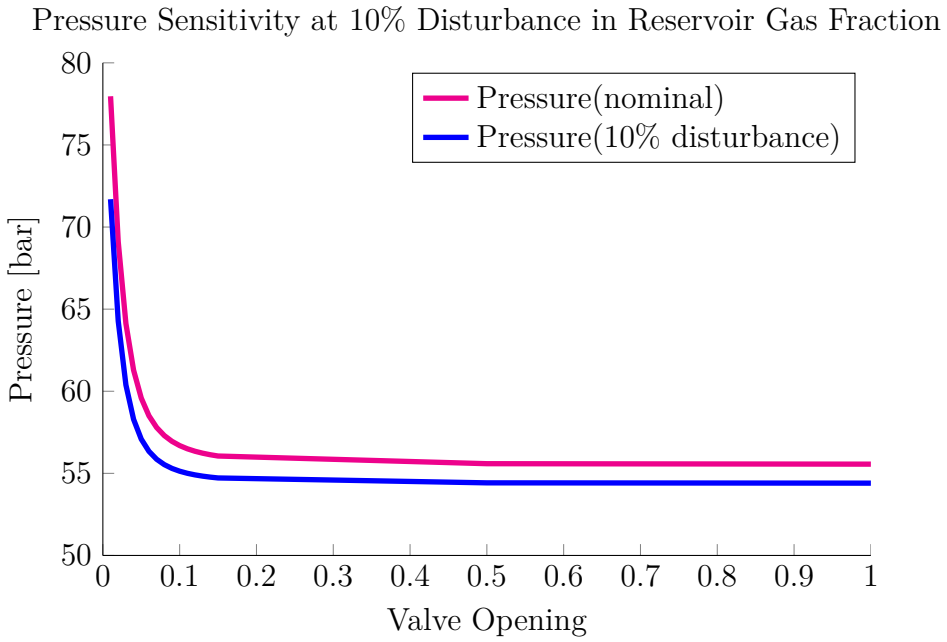

Figure 3: The wellhead pressure as a function of valve opening at nominal values, and at 10% disturbance in the reservoir gas fraction.

1 bar. This result is reasonable as the pressure is a function of the density of the mixture, which will change as the gas composition increases.

4.2.2 Conclusion of Sensitivity Test

The results in section 4.2.1 implies that the wellhead pressure is affected by a shift in the GOR. This is reasonable as the density of the mixture is a function of the gas composition. From these results we find that it is interesting to investigate the potential for the wellhead pressure as a self-optimizing variable in our system, and therefore also to continue the developing of the MATLAB-model.

Part II

Method

To investigate the wellhead pressure as a self-optimizing variable, we wish to make a model of our system that can be optimized. For this purpose, MATLAB is considered a good tool. In order to verify the flow and pressure relations in this model, a similar model is made in OLGA. OLGA is a modelling tool for multiphase transport of oil, gas and water through pipelines, and is established as a world leading product in this field.

From OLGA-simulations we obtain data for the flow- and pressure behaviour at different valve openings and in different parts in the pipeline. In this theses we attempt to describe this data by applying basic physical principles to develop a simple MATLAB-model.

5 The OLGA Model

Data from the Troll West structure and the work of Gunnerud and Foss(2009) is used as a basis for the model. The model consists of four wells, which are set to produce similar amounts of oil, water and gas as the four wells from the Troll-dataset given in appendix A. A figure of the OLGA model is presented in Figure 4.

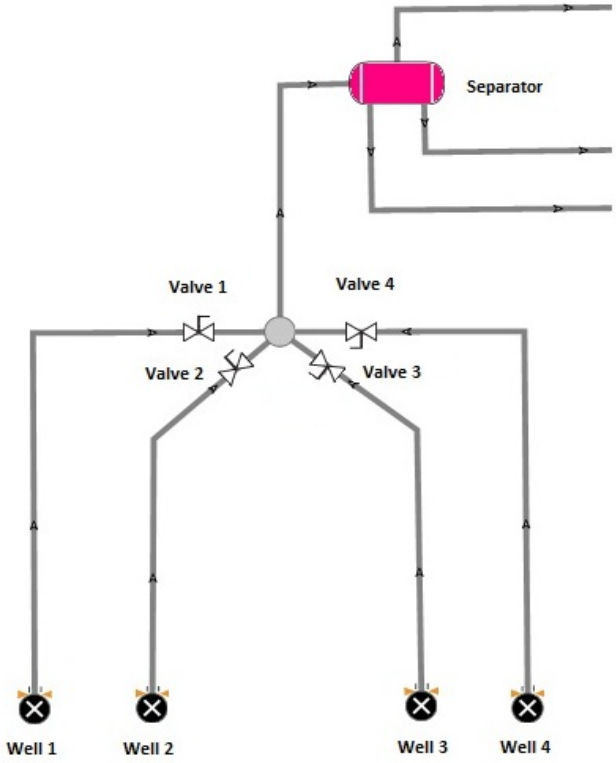

Figure 4: An illustration of the OLGA model.

5.1 Well and Pipe Specifications

The software OLGA is used to simulate Typical well and reservoir conditions. The specifications for the wells and pipes are listed in are listed in table 1 and 2 respectively.

Table 1: Well Specifications

	Well 1	Well 2	Well 3	Well 4
Well Depth $[m]$	1300	1200	2000	1000
Well Pressure $[bar]$	205	195	250	180
Well Temperature $[C^o]$	63	60	80	55
Gas Fraction	0.09	0.1	0.08	0.1
Water Fraction	0.63	0.6	0.7	0.57

In Table 1 we see that the four wells are at different depths in the reservoir, and have different temperatures and pressures as a result to this. Because of homogeneity in the reservoir formation, which means that there is an uneven distribution of pores and concentrations of petroleum mixture, the composition of water, gas and oil also changes.

Table 2: Pipe Specifications

	Pipe 1	Pipe 2	Pipe 3	Pipe 4
Pipe Length $[m]$	1300	1200	2000	1000
Inner Pipe Diameter $[m]$	0.1	0.1	0.1	0.1
Roughness $[m]$	$1 \cdot 10^{-5}$	$1 \cdot 10^{-5}$	$1 \cdot 10^{-5}$	$1 \cdot 10^{-5}$

The physical specification of the four pipelines are given in Table 2.

The same model is used for all four valves and the physical specifications are given in Table 3. Valve specifications that are only needed for the OLGA model are given in appendix B.

Table 3: Valve Specifications*

	Diameter [m]	C_f-factor[-]
Valve 1(-4)	0.0762	0.84

* The remaining valve specifications is only needed for the OLGA model, and will be given in appendix B.

As the valve opening often is the only variable that can be directly manipulated in an oil well, it is important that we map how changing this parameter will affect the operation. There is therefore gathered much data from simulations of this type, and the most relevant tables are included in appendix C. The MATLAB-model should give information on how flow and pressure conditions change as a function of the valve opening, as this is important properties when a well-network is optimized.

5.2 The OLGA Software

OLGA is a modelling tool for multiphase transport of oil, gas and water through pipelines, and is established as a world leading product in this field. The software has enabled the development of deep see oil and gas fields that would not be possible without this technology.

OLGA is a powerful tool for design and operation when considering new or existing installation. It also has applications for control and tuning. The software, however, has no application for optimization. In investigating this problem it would be desirable to use a tool with high accuracy for flow and reservoir simulations, as well as having the possibility for optimization. Based on flow simulations from OLGA a simple flow model will be implemented in MATLAB where it can be combined with various optimization routines.

Part III

Model Development

Developing the MATLAB-model, data from only one of the wells is used. The well that is used for the model is well 1, and the physical data for this well can be found in Table 1. An illustration of the pipeline that will be modelled in our MATLAB-model is presented in Figure 5.

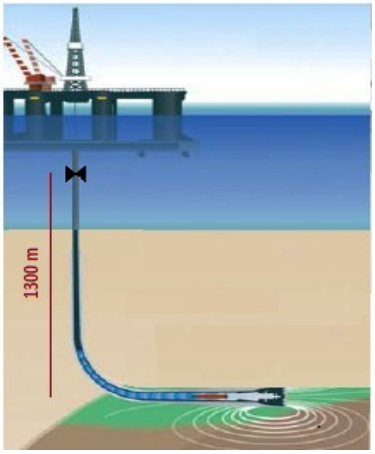

Figure 5: The well that is described our model.

The MATLAB-model consists of three different flow-models;

1. Inflow from reservoir
2. Flow relations in pipe
3. Flow relations through valve

These flow models are based on different principles and theory, and are modelled separately. In the finished model, the parts are connected together and made a function of the valve opening, as this often is the only variable that can be manually manipulated in a well.

6 Inflow Model

6.1 Inflow Theory

To simulate the fluid flow from the reservoir into a well, the equation below is used:

$$P_w = P_e - \underbrace{\frac{\mu\left(ln\frac{r_e}{r_w} + S\right)q}{2\pi kh}}_{\text{Constant}} \tag{1}$$

In Equation 1 the fluid flow(q) is given in $\left[\frac{m^3}{s}\right]$ and is a linear function of the pressure difference between the well(P_w) and the reservoir boundary(P_e). All pressures are given in $[Pa]$. The equation is derived from *Darcy's Law* as will be elaborated upon in section 6.1.1.

The size of the constant depends mainly on reservoir- and fluid properties. These properties are; the ratio of the distance between the well(r_w) and the reservoir boundary(r_e); the permeability(k) which has the unit $[m^2]$; the formation thickness(h) and the viscosity(μ) of the fluid which is given in $\left[\frac{kg}{ms}\right]$. The constant also contains a skin factor(S) to account for reduced permeability (and, thus, reduced flow) in the region near the well. The reduced permeability is a result of the damage made to the formation during the drilling of the well and will be further explained in section 6.1.2.

6.1.1 Darcy's Law

Darcy's law describes flow through porous media, like the one in a petroleum reservoir. Darcy established that the flow velocity was directly proportional with the pressure difference across the porous media for any given flow. For radial flow, Darcy's law is given in Equation 2:

$$u = \frac{k}{\mu}\frac{dP}{dr} \tag{2}$$

The flow velocity(u) is given in$\left[\frac{m}{s}\right]$. Darcy's law was originally an empirical expression based on observations and experiments, but later Hubbert(1956) managed to derive the law directly from Navier-Stokes equation of motion of viscous fluids. For details on this derivation, see King Hubbert(1956).

This mathematical description of the radial flow of fluids through a porous media simulates flow from a reservoir into the wellbore. Figure 6 presents a typical pressure profile from the outer boundary of the reservoir(r_e) to the well(r_w).

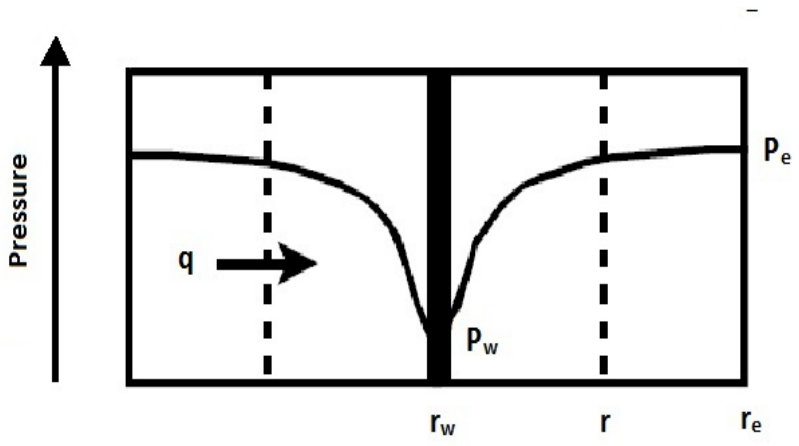

Figure 6: The radial flow of oil into a well under steady state flow conditions.

The model applies to a reservoir at steady state condition. For the sake of simplicity the reservoir is assumed to be homogeneous, i.e it is assumed to be no gradients in permeability or other reservoir parameters.

Assuming that the fluid is incompressible, the velocity can be expressed as in equation 3:

$$u = \frac{q}{A} \tag{3}$$

By rearranging Equation 2 and substituting A with the expression for a radial area, A= $2\pi rh$, the equation can be written:

$$\frac{dP}{dr} = \frac{q\mu}{kh2\pi r} \tag{4}$$

Separating the variables and integrating Equation 4 gives:

$$P - P_w = \frac{q\mu}{kh2\pi} ln \frac{r}{r_w} \tag{5}$$

This equation shows that the pressure increases logarithmically with respect to the radius, i.e the pressure drop being more severe close to the well(r_w) than towards the outer boundary(r_e). Using boundary conditions $r = r_e$ and $P = P_e$, the flow(q) from a reservoir into an oil well can expressed as follows:

$$q = \frac{2\pi kh}{\mu ln \frac{r_e}{r_w}} (P_e - P_w) \tag{6}$$

6.1.2 Skin factor

When a well is being drilled, it is common that some of the drilling mud will flow into the formation and partially plug the pore spaces. This will reduce the permeability in the formation near the well, and thus, reduce the flow in this area.

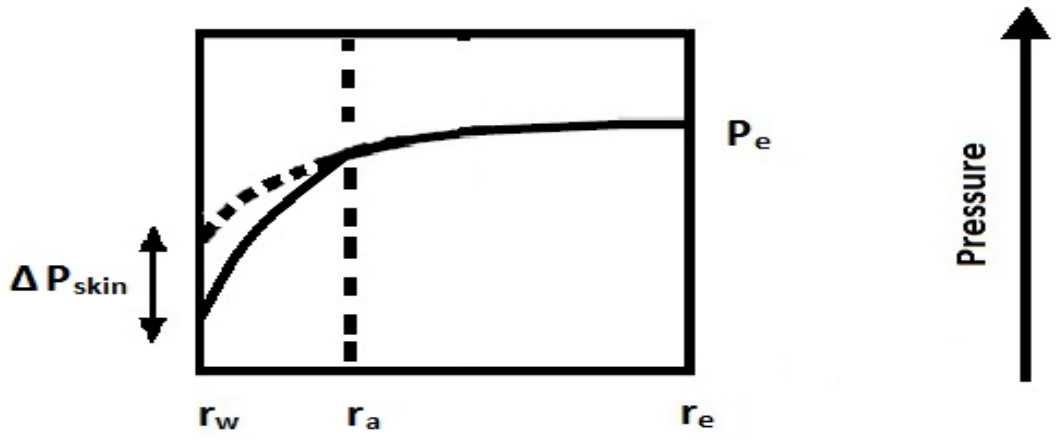

Figure 7: The radial pressure profile for a damaged well.

Figure 7 compares the pressure profile in a damaged well with the pressure profile in an undamaged well. The area $r \leq r_a$ represent the damaged zone. If the well was undamaged the pressure drop for $r < r_a$ would be represented by the dashed line. Due to the reduced permeability in a damaged well, the pressure drop in the damaged zone will be larger than normal. This additional pressure drop is denoted $\triangle P_{skin}$ with the definition:

$$\triangle P_{skin} = \frac{q\mu}{2\pi kh} S \tag{7}$$

Here, S is the dimensionless mechanical skin factor. The size of this factor depends on the magnitude of the damage made to the well. This can be checked by performing various well tests, but will not be elaborated upon in this thesis.

6.2 Results and Discussion

6.2.1 Flow profiles

By plotting simulation data of the flow from the reservoir into the the well, we can confirm that there is a linear relationship between the flow and the pressure difference between the reservoir and the bottom hole pressure.In Figure 8 the flow is plotted as a function of the bottom hole pressure. The reservoir pressure is assumed to be constant.

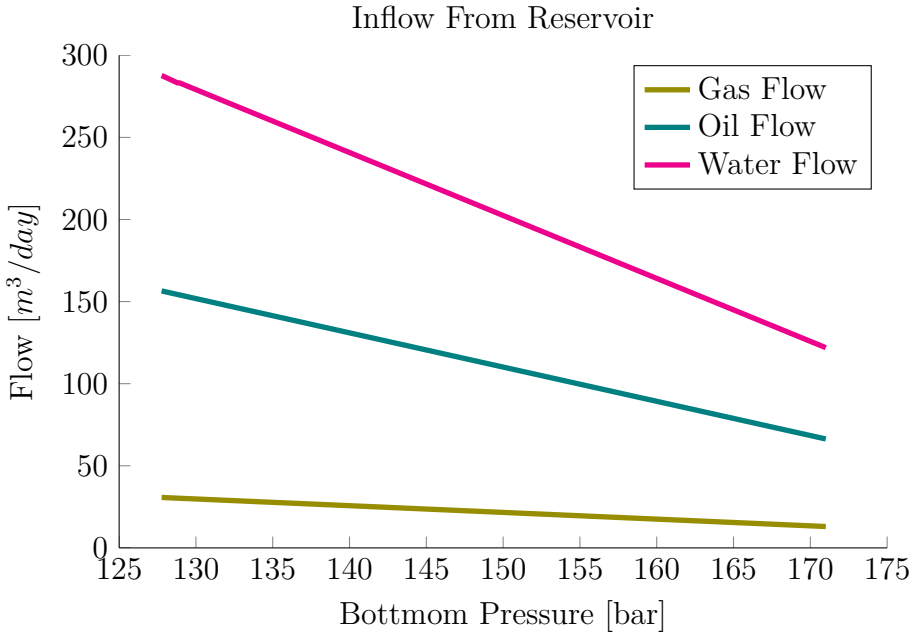

Figure 8: The flow from the reservoir into the well as a function of bottom pressure. The flow is given in *standard* m^3.

The flow profiles showed in Figure 8 indicates that Equation 1 can be used to model the inflow in our system, as this equation describes *linear* flows. The flow is given in *standard* m^3, which is the volume flow at standard conditions(T= 273.15 [K] P=1[bar]).

Figure 9 shows the bottom hole pressure as a function of valve opening. We see that for valve opening 0.01 to 0.1 the bottom hole pressure decreases from 170 bar to 130 bar. For valve openings between 0.1 and 1, the value of the bottom hole pressure flattens out at approximately 128 bar.

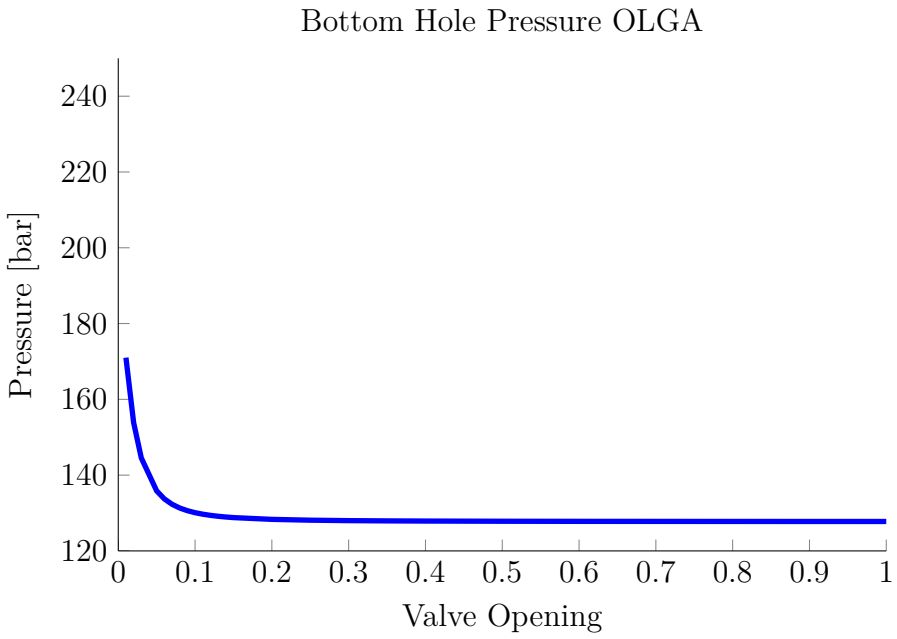

Figure 9: Bottom hole pressure as a function of valve opening. The data is generated from simulations in OLGA.

In Figure 10 we compare pressure estimated form Darcy's law with the bottom hole pressure from Figure 9.

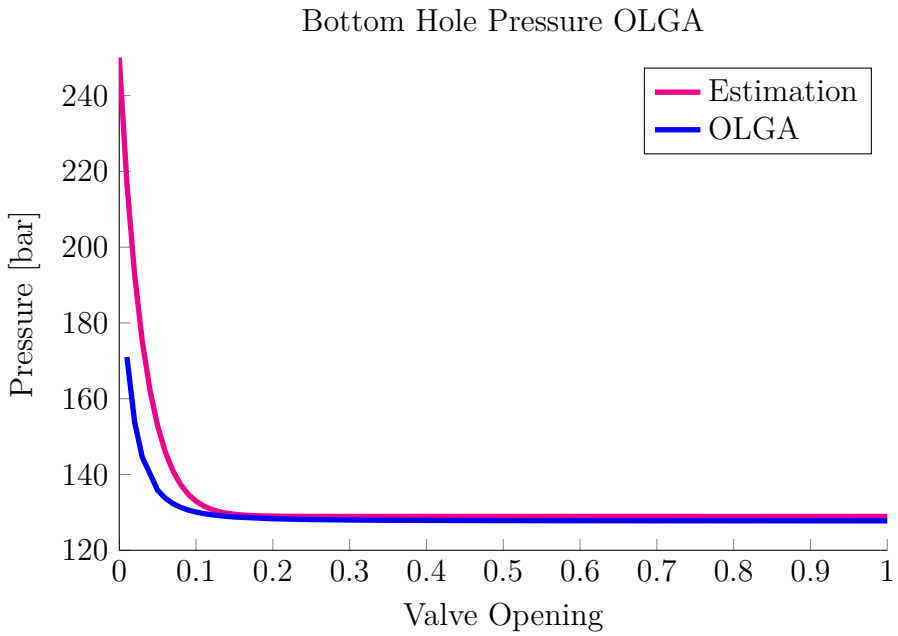

Figure 10: A comparison of the estimated bottom hole pressure and the bottom hole pressure generated in OLGA.

We see that Darcy's law gives a quite good estimation for the bottom hole pressure in our system, but that the estimation is generally poorer at valve openings between 0 and 0.15.

7 Pipe Flow Model

The pressure- and density profile in the pipe is calculated with a basis in the compressibility equation of state:

$$PV = znRT \tag{8}$$

Here, pressure(P) is given in $[bar]$, volume (V) is given in $[m^3]$, n denotes the number of moles and the temperature(T) is given in $[K]$. The gas constant(R) has the value $8.3144 \cdot 10^{-5}$ $\left[\frac{barm^3}{moleK}\right]$.

The steps of calculating the z-factor in Equation 8 are described in the book of McCain (1990), and will be presented in the following sections.

7.1 Pipeflow Theory

This equation is also known as the *real gas equation* and has a correction factor, z, to account for the deviation from ideal- to real gas behaviour. The correction factor is known as the *compressibility factor* and is the ratio of the volume actually occupied by a gas at a given pressure and temperature, to the volume the gas would occupy at the same pressure and temperature if it had behaved like an ideal gas.

$$z = \frac{V_{actual}}{V_{ideal}} \tag{9}$$

Typically, a real gas behaves similarly to an ideal gas at low pressures and also as the actual occupied volume approaches the ideal volume. At these conditions the compressibility factor will have a value close to *one*, as illustrated in Figure 11.

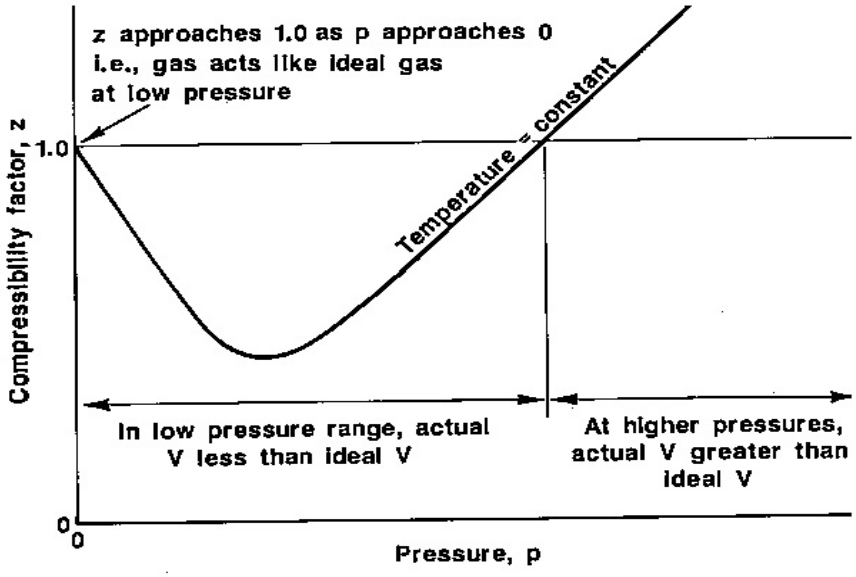

Figure 11: The typical shape of a z-factor curve as a function of pressure at constant temperature.

To find the compressibility factor at the bottom of the reservoir, the gas formation factor B_g is calculated. The factor relates the volume of 1 lbmol of gas at reservoir conditions to the volume of the same lbmol of gas at standard conditions. This gives gives:

$$B_g = \frac{\widehat{v}^{res}}{\widehat{v}^{STP}} = \frac{\rho^{STP}}{\rho^{res}} \tag{10}$$

By inserting equation8 B_g can be expressed as follows:

$$B_g = \frac{\frac{P^{STP}}{RT^{STP}z^{STP}}}{\frac{P^{res}}{RT^{res}z^{res}}} \tag{11}$$

Pressure and temperature at standard conditions are $1.013\,[bar]$ ($1\,[atm]$) and $273.15\,[K]$ respectively. The compressibility factor z is assumed to be 1 at standard conditions. This results in an expression for B_g as presented in

equation 12:

$$B_g = 0.003354 \frac{T_{res} z_{res}}{P_{res}} \tag{12}$$

The compressibility factor must be determined experimentally and varies with changes in temperature, pressure and composition. A chart of z-factors for natural gas is given in Figure 12. The compressibility chart was presented by Standing and Katz(1942), and is a widely accepted correlation in petroleum industry. The chart in Figure 12 relates pseudoreduced pressure(P_{pr}) and pseudoreduced temperature(T_{pr}) to the z-factor of the gas.

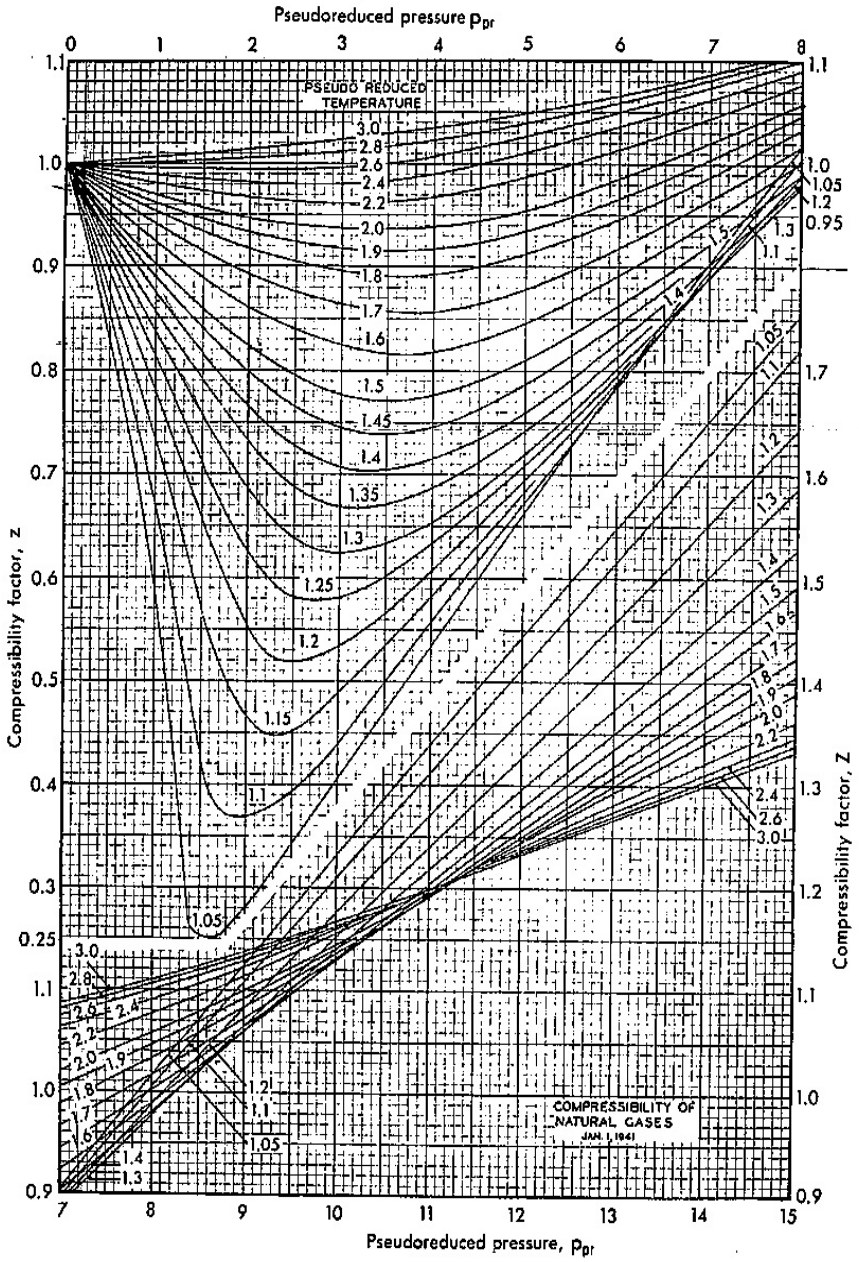

Figure 12: Compressibility factors of natural gases. From Standing and Katz(1942)

7.1.1 Law of Corresponding States

The discovery that, for most gases, the isotherms are very similar has led to the development of the *Law of Corresponding States* and the definition of reduced pressure (P_r) and reduced temperature (T_r). The definitions are given in Equation 13 and 14 respectively, where the critical pressure and temperature of the gas are denoted P_c and T_c.

$$P_r = \frac{P}{P_c} \tag{13}$$

$$T_r = \frac{T}{T_c} \tag{14}$$

The law correlates pure gases so that at the same reduced pressure and reduced temperature, all gases will have the same z-factor.

The Law of Corresponding States was originally made for pure gases, but has been extended to also cover mixed gases, like the natural gas in a petroleum reservoir . As obtaining the critical values for a multicomponent mixture is complicated,*pseudoreduced* pressure(P_{pr}) and *pseudoreduced* temperature(T_{pr}) has been defined as:

$$P_{pr} = \frac{P}{P_{cr}} \tag{15}$$

$$T_{pr} = \frac{T}{T_{cr}} \tag{16}$$

Here, P_{cr} and T_{cr} are pseudocritical pressure and temperature for mixed gas.

7.1.2 Compensation for Non-hydrocarbon Components

Natural gas commonly contains some non-hydrocarbon components as hydrogen sulphide, carbon dioxide and nitrogen. Especially the presence of hydrogen sulphide and carbon dioxide can cause errors in the calculated z-factor if not accounted for.

The equations for this adjustment are given in equations 17 and 18:

$$P'_{pc} = \frac{P_{pc}T'_{pc}}{T_{pc} + y_{H_2S}(1 - y_{H_2S})\epsilon} \tag{17}$$

$$T'_{pc} = T_{pc} - \epsilon \tag{18}$$

The pseudocritical temperature adjustment factor,ϵ , is obtained from equation 19 - 21 where y_{CO_2} and y_{H_2S} denotes the mole fraction of CO_2 and H_2S. Nitrogen is not included as it is assumed to have no significant effect on the z-factor.

$$\epsilon = 120(A^{0.9} - A^{1.6}) + 15(B^{0.5} - B^4) \tag{19}$$

$$A = y_{CO_2} + y_{H_2S} \tag{20}$$

$$B = y_{H_2S} \tag{21}$$

Pseudocritical pressure P_{pc} and pseudocritical temperature T_{pc} are calculated by the empirical equations 22 and 23 :

$$P_{pc} = 756.8 - 131\delta_g - 3.68\delta_g^2 \tag{22}$$

$$T_{pc} = 169.2 - 349.5\delta_g - 74.0\delta_g^2 \tag{23}$$

In Equation 22 and 23, δ_g denotes specific gravity of gas(in this case natural gas) at standard conditions:

$$\delta_g = \frac{M_g}{M_{air}} \tag{24}$$

7.1.3 Mixed Density

The density of the mixture is calculated by equations 25- 27. In the equations v_i denotes the *volume fraction* of component i in the mixture and ρ_i is the density of the pure component i.

$$\rho_{mix} = \sum_i v_i \rho_i \tag{25}$$

The volume fraction v_i is calculated by Equation 25, where V_i is the volume of the component, and V_{tot} is the total volume of the mixture.

$$v_i = \frac{V_i}{V_{tot}} \tag{26}$$

The density of the component i is calculated by Equation 27, where M_i is the molar weight of component i.

$$\rho_i = \frac{PM_i}{RT} \tag{27}$$

7.1.4 Pressure and Density correlation

Pressure and density is correlated by Equation 28.

$$P = \rho g h \tag{28}$$

7.2 Results and Discussion

7.2.1 Pressure Profile

Figure 13 shows how the pressure in the pipe decreases from 129.3 bar in the bottom hole, to 50.8 bar at the valve. The pressure profile is generated from data obtained from OLGA-simulations, which were made at valve opening 0.2.

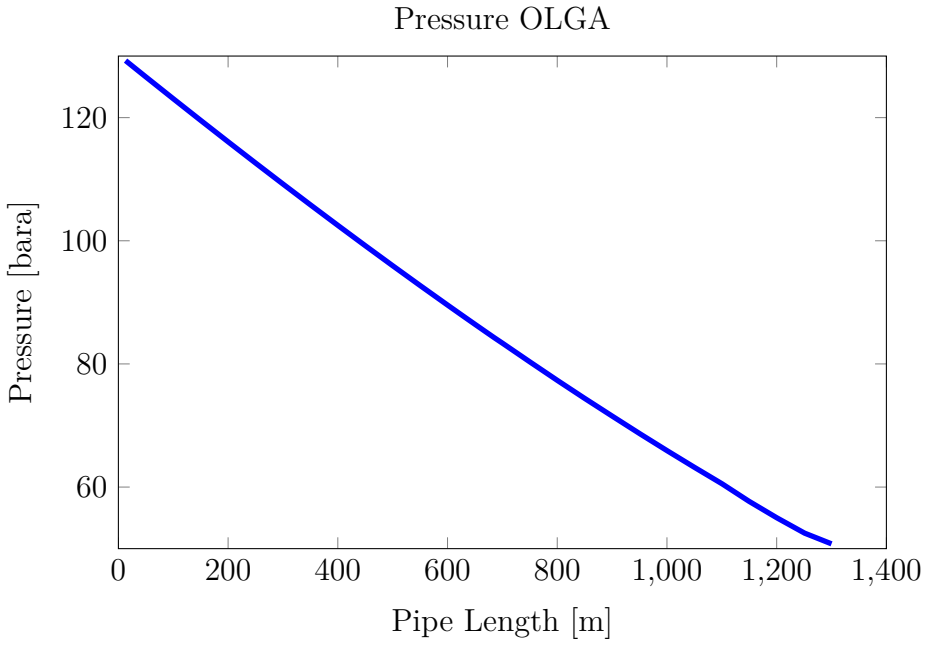

Figure 13: The pressure profile in the pipe as a function of pipe length. The data is obtained from OLGA.

As expected, the results in Figure 13 show a correlation between the pressure in the pipe and depth below sea level. However, the pressure profile is not linear, but slightly curved. This means that the pressure cannot only be a

linear function of the elevation in the pipe and that also the variation in density must be taken into account when making a model for the pressure drop.

Figure 14 compares the estimated pressure profile and the pressure profile from Figure 13. The estimation of the pressure profile is calculated from Equation 28. As discussed in the previous section, the density of the mixture will decrease significantly. Therefore, the density (ρ) in Equation 28 is also calculated as function of the height in the pipe.

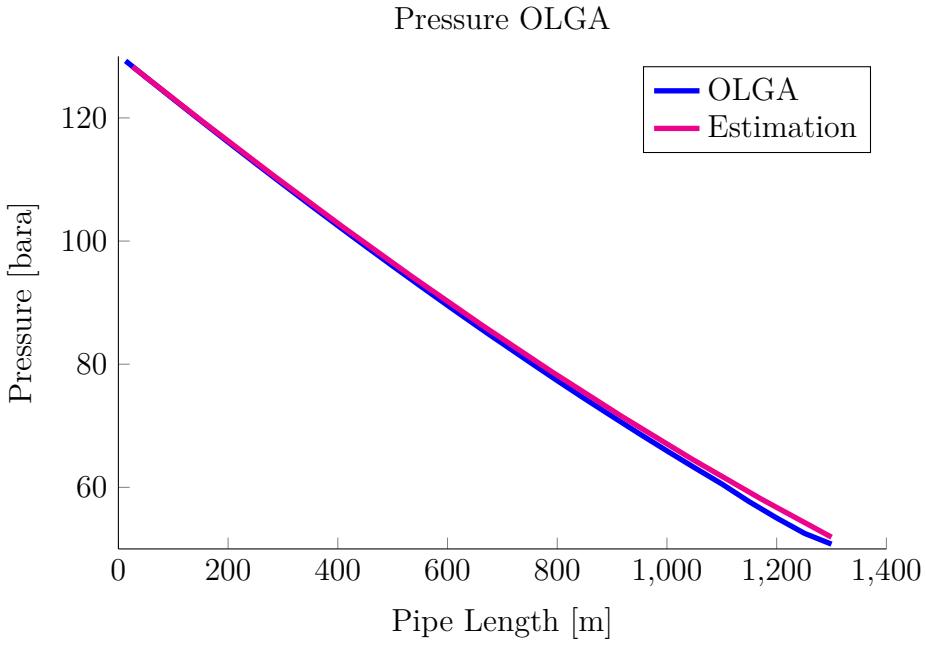

Figure 14: A comparison of the estimated pressure profile in the pipe with the pressure profile from OLGA.

The trends in the pressure profile from OLGA and the estimated profile are very similar. Approaching the valve, there is a slight deviation of 1 bar between the real vales and the estimation.

7.2.2 Density Profile

Figure 15 show how the density of the petroleum mixture decrease from 699.4 $\left[\frac{kg}{m^3}\right]$ in the bottom of the pipe to 445 $\left[\frac{kg}{m^3}\right]$ at the valve. The density of the mixture decreases the higher up in the pipe it flows. The trend is not linear, but slightly curved. The density profile is generated from data obtained from OLGA-simulations, which were made at the valve opening 0.2.

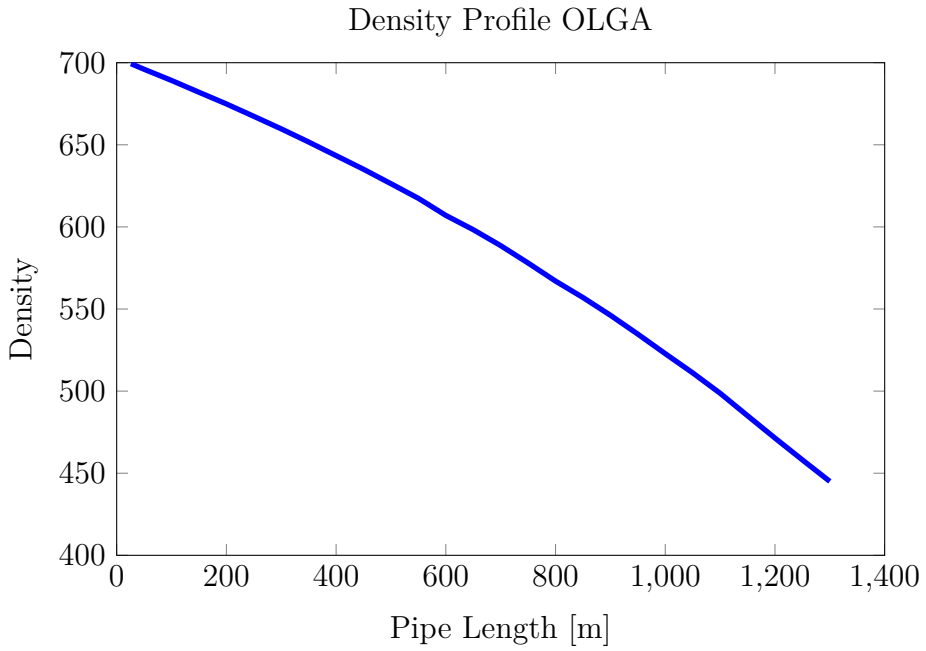

Figure 15: The density profile as a function of the pipe length. The data is obtained from OLGA.

Figure 16 compares the estimated density profile with the density profile from Figure 15, and it shows that with increasing pressure, the density of the fluid increase. This is because the molecules in a compressible fluid will be pressed tighter together at a higher presser, which will increase mass per volume. As oil and water are assumed to be incompressible fluids, the changing pressure will only have effect on the density of the gas component in the mixture. The density of the gas is calculated by the 27 and the density of the mixture is then calculated by Equation 25.

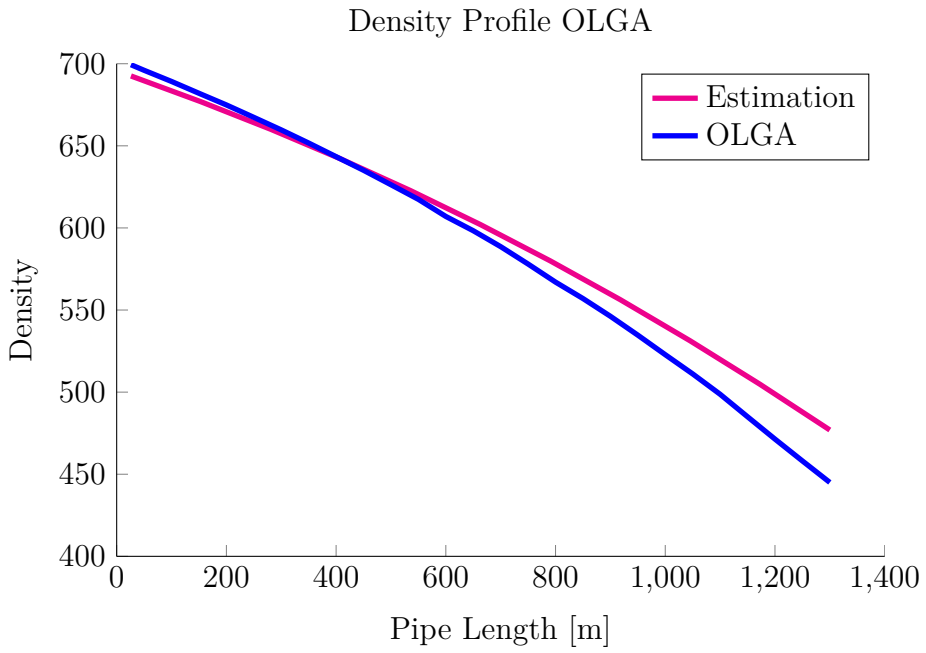

Figure 16: A comparison of the estimated density profile and the density profile from OLGA.

As seen in Figure 16, the trends in the density estimation are quite similar to the real values. When approaching the valve, however, the deviation increases. Because the density estimation is based on the estimation of the pressure, there is a correlation between the deviations in these two estimates.

It is reasonable to assume that an improvement in one of the models automatically will give an improvement in the other model. Some of the deviation in the density estimate can therefore be explained by the deviations in the estimate of the pressure.

8 Valve Model

8.1 Valve Theory

The pressure drop across a valve is difficult to model, as the fluid dynamic in the valve is very complex. Many calculations of pressure drop and flow through a valve are therefore based on equations that are highly empirical. In the following sections we will describe two different methods on how to model the pressure drop across the valve in our system. The first method is based on empirical models , the latter is based on Bernoulli's equation, and is also the method which is used in OLGA.

8.1.1 Pressure Drop Calculations using Bernoulli

Equation 29 is used to model the pressure drop across the valve. The model is derived from Bernoulli's equation, which will be shown in the next section.

$$\triangle P_{Valve} = \frac{1}{2}\rho \left(\frac{Q}{A_A}\right)^2 \left[\frac{1 - C_f^2}{(ZC_f)^2}\right] \tag{29}$$

Here A_A represent the cross-sectional area of the valve inlet, and Z the valve opening at the orifice. As the pressure in the pipe vary as a function of the valve opening, the values of the volume flow (Q) and the density (ρ) also need to be calculated for each valve opening. The density *through* the valve, is assumed to be constant. In this model we assume the flow through the valve to have the same characteristics as illustrated in Figure 17.

Derivation from Bernoulli

Equation 29 is derived from the incompressible Bernoulli's equation presented below:

$$\int_1^2 \frac{dP}{\rho} = \int_1^2 U dU \tag{30}$$

Integrating Equation 30 gives:

$$\triangle P = \frac{1}{2}\rho(U_2)^2 - \frac{1}{2}\rho(U_1)^2 \tag{31}$$

Here ρ is the mixed density in $\left[\frac{kg}{m^3}\right]$ and U is the fluid velocity in $\left[\frac{m}{s}\right]$.
It follows from continuity that:

$$U = \frac{Q}{A} \tag{32}$$

where Q represents the volume flow given in $\left[\frac{m^3}{s}\right]$, and A, the flow area in $[m^2]$. Thus, the pressure drop can be expressed:

$$\triangle P = \frac{1}{2}\rho\left(\frac{Q}{A}_2\right)^2 - \frac{1}{2}\rho\left(\frac{Q}{A}_1\right)^2 \tag{33}$$

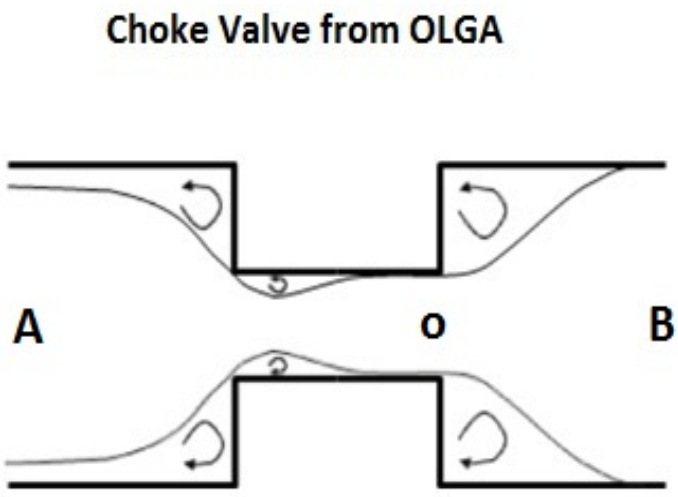

Figure 17: An illustration of the flow through a vale from position A, through the orifice (o), to position B.

We divide the calculation of the pressure drop across the vale in two, and calculate; the pressure drop from position A to orifice (o), and pressure recovery from orifice to position B. Finally, the two contributions are added to find the pressure drop from position A to position B.

$$\triangle P = \triangle P_{A,o} + \triangle P_{o,B} = \int_A^o \rho U dU + \int_o^B \rho U dU \tag{34}$$

Pressure Drop from Inlet to Orifice

As illustrated in Figure 17, the flow conditions at the orifice makes the *efficient flow area* smaller than the cross sectional area of the orifice. To account for this effect, a discharge coefficient(C_f) is introduced.

$$\triangle P_{A,o} = \frac{1}{2}\rho\left(\frac{Q}{A_o C_f}\right)^2 - \frac{1}{2}\rho\left(\frac{Q}{A}_A\right)^2 \tag{35}$$

The coefficient C_f is the ratio between cross sectional area of the orifice and the efficient flow area.

$$C_f = \frac{A_o^{eff}}{A_o} \tag{36}$$

The ratio $\frac{A_2}{A_1}$ can be expressed by the valve opening Z, and thus the pressure drop can be expressed as in Equation 37.

$$\triangle P_{A,o} = \frac{1}{2}\rho\left(\frac{Q}{A_A}\right)^2\left[\left(\frac{1}{ZC_f}\right)^2 - 1\right] \tag{37}$$

Pressure Recovery

Due to area extension, which causes the pressure recovery between the orifice and position B, the pressure drop will be reduced in this part of the valve. Again, we use Bernoulli's equation, given in 30 and integrate from orifice to position B. The loss of effective flow area, is accounted for in the first part of the valve, and does therefore not need to be accounted for here.

$$\triangle P_{o,B} = \frac{1}{2}\rho\left(\frac{Q}{A_A}\right)^2\left[1 - \left(\frac{1}{Z}\right)^2\right] \tag{38}$$

The valve inlet has the same cross-sectional(A_A) as the cross-sectional area of the valve outlet(A_B). By combining the two pressure drop calculations (equation 38 and 37) and setting $A_B = A_A$, we get an expression for the total pressure drop across the valve as written in Equation 39.

$$\triangle P_{A,o} + \triangle P_{o,B} = \frac{1}{2}\rho\left(\frac{Q}{A_A}\right)^2\left[\left(\frac{1}{ZC_f}\right)^2 - \left(\frac{1}{Z}\right)^2\right] \tag{39}$$

8.1.2 Pressure Drop Calculations using Valve Equation

In the second method for doing the pressure drop calculations across the valve, is by using Equation 40

$$\triangle p = \rho\left(\frac{q}{C_d f(z) A}\right)^2 \tag{40}$$

which is derived from the *Valve Equation*, given in Equation 41.

$$q = C_d f(z) A\sqrt{\frac{\triangle p}{\rho}} \tag{41}$$

The valve equation describes the flow dependency as a function of valve opening and the pressure drop across the valve. (ref. Boken til Skogestad). Here, the volume flow is q, and C_d is the dimensionless valve coefficient. The cross-sectional area of the valve (inlet or outlet) is represented by A , $\triangle P$ is the pressure drop from valve inlet to valve outlet, and ρ denotes the density of the fluid. The function f(z) is the inherent valve characteristics, and will be elaborated upon in the next section.

Valve Characteristics

All valves have an inherent valve characteristic which describes the relationship between the valve capacity and the flow through the valve. In the book of Buckley (1964), he describes different valve types and their flow characteristics. It is the different physical dimensions of the valve that affects the flow characteristic as a function of valve opening. Valve dimensions are often customized, so that the flow characteristic meets the customers control needs.

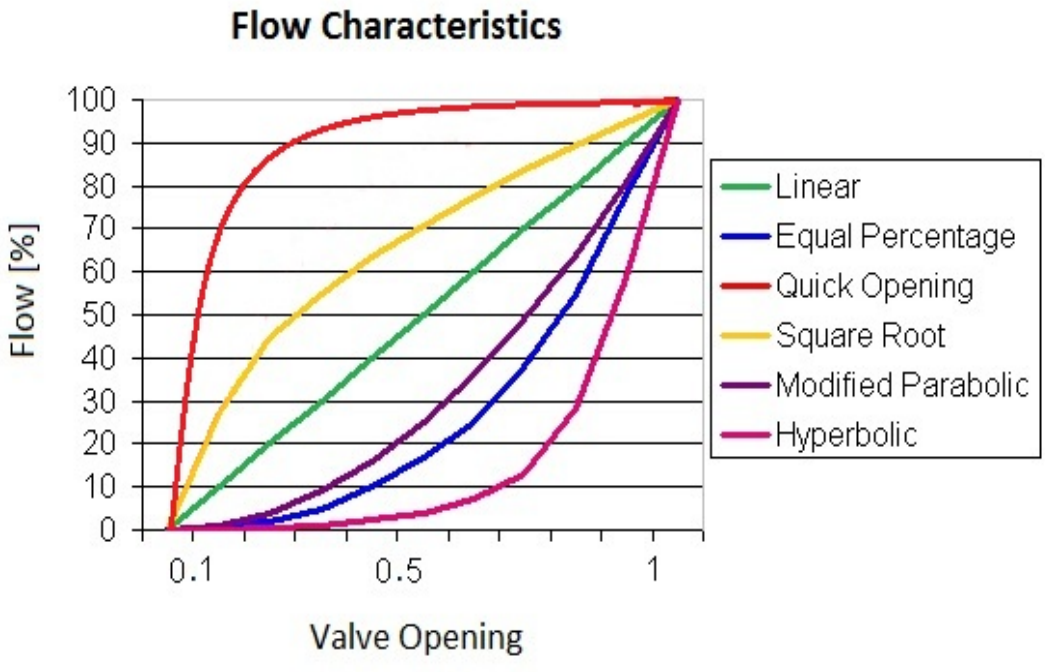

Figure 18: Inherent flow characteristics of different control valves.

Figure 18 shows some common valve characteristics, plotted as percent of the maximum flow through the valve as a function of valve opening.

Most valves used in control applications are:

Linear Valve Control $f(z) = z$
The flow is directly proportional with valve opening. Increasing valve opening gives a linear increase in flowrate.

Equal Percentage Control $f(z) = log(z)$
As the valve opening increases the flowrate increase with a certain percent of the previous flow. The relationship between the valve opening and the flowrate is logarithmic.

Quick Opening Control
This design of a Quick Opening Valve gives a large increases in flow for small changes in valve opening from the closed position. In contradiction to a linear valve and a equal percent valve, the exact shape of the characteristic curve is not defined. Both a valve giving 90% flow at 10% valve opening, and a valve giving 90% at 60% valve opening can be characterised as a quick opening valve.

By identifying the flow characteristic of the valve in our system, and applying it in Equation 40, this can give an accurate estimate of the of the pressure drop.

8.2 Result and Discussion

The following sections will present the results from flow-, and valve characteristics as well as the pressure drop estimations calculated by both the Valve Equation Approach and the Bernoulli Approach.

8.2.1 Flow Characteristics

In order to determine the flow characteristics of the valve in our system, the flow rate was plotted as a function of valve opening. The result is presented in Figure 19.

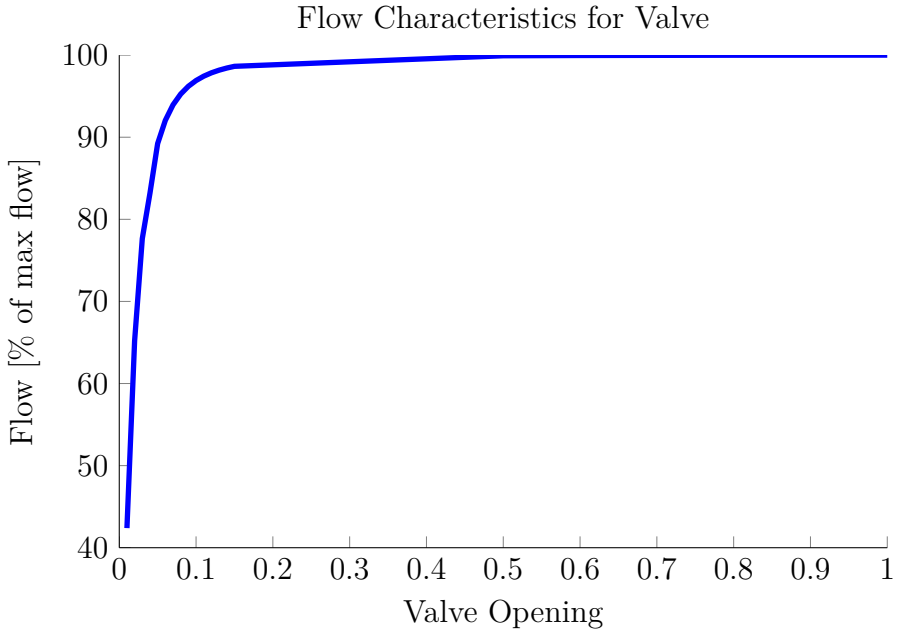

Figure 19: Flow characteristics for the valve.

The flow characteristics in Figure 19 resembles the trends of a *quick opening valve*. Here, a small change in valve opening gives a large increase in flowrate

for valve openings between 0 and 0.1, and a lagre change in valve opening gives a small increase in flowrate for valve openings between 0.1 and 1.

As mentioned in section 8.1.2, quick opening characteristics does not have any defined standard shape, and the function must be adjusted to the specific characteristic. It is therefore difficult to derive a function for the valve characteristics directly from the flow characteristics in Figure 19. From simulations in OLGA, we have values for the pressure drop across the valve at different valve openings, thus, we can plot the characteristic function and use this to adjust estimate a function for the valve characteristic.

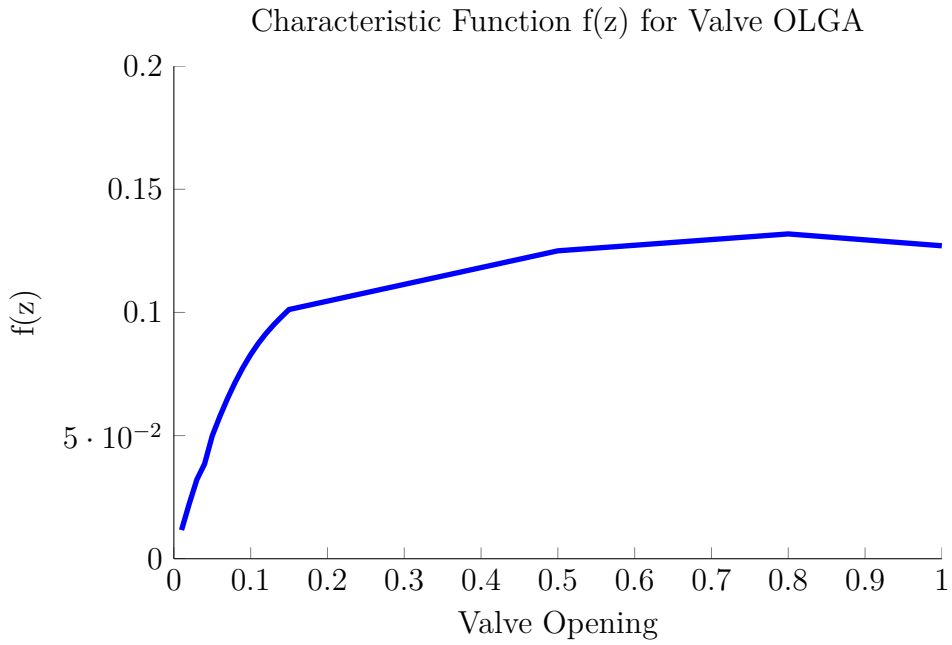

Figure 20: Characteristic function for the valve.

The valve characteristics, f(z), obtained from OLGA simulations is plotted in Figure 20. The valve characteristics resembles an exponential function, and by the trial and error approach the function is set to:

$$f(z) = 0.13(1 - exp(-9z))$$

A comparison of the estimation and the real value of the valve characteristics is presented in Figure 21.

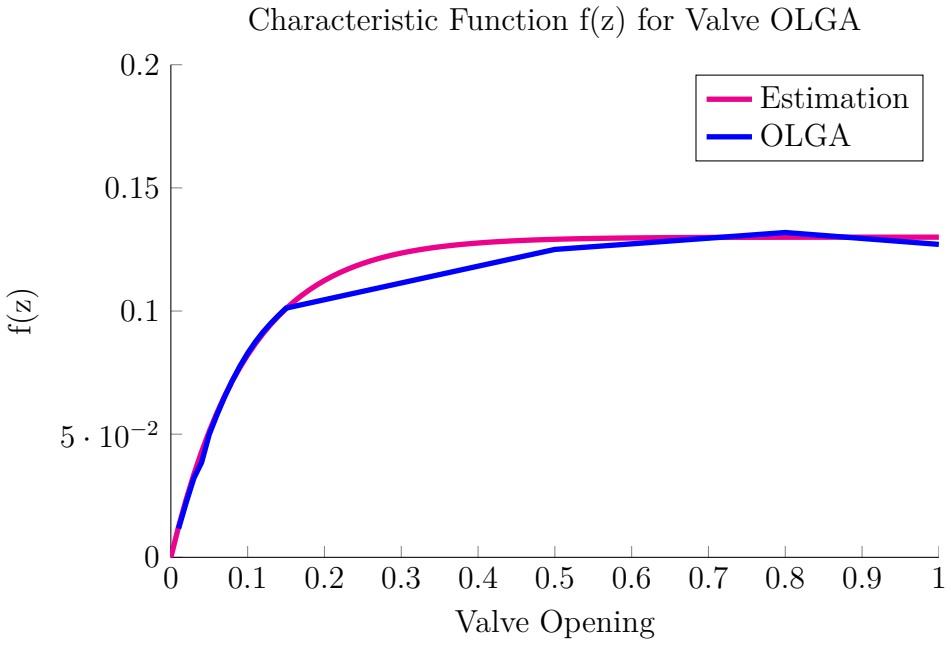

Figure 21: Comparison of theestimated characteristic function and the characteristic function for the valve.

We see from Figure 21 that the exponential function fails to describe the valve characteristics completely, but gives an acceptable estimation. This should be kept in mind when later looking at the pressure drop estimation. However, this is the function used as f(z) in the vave equation when estimating the pressure drop across the valve in section 8.2.2.

8.2.2 Pressure-drop Profiles

Figure 22 shows the pressure drop across the valve as a function of valve opening. The pressure drop profile is generated from data obtained from OLGA-simulations. As we see from the figure, the pressure drop only becomes large for small valve-openings(< 0.05), and is very flat for the larger valve openings. From valve opening 0.1 to 1.0 the pressure drop only decreases from 3.05 bar to 1.35 bar.

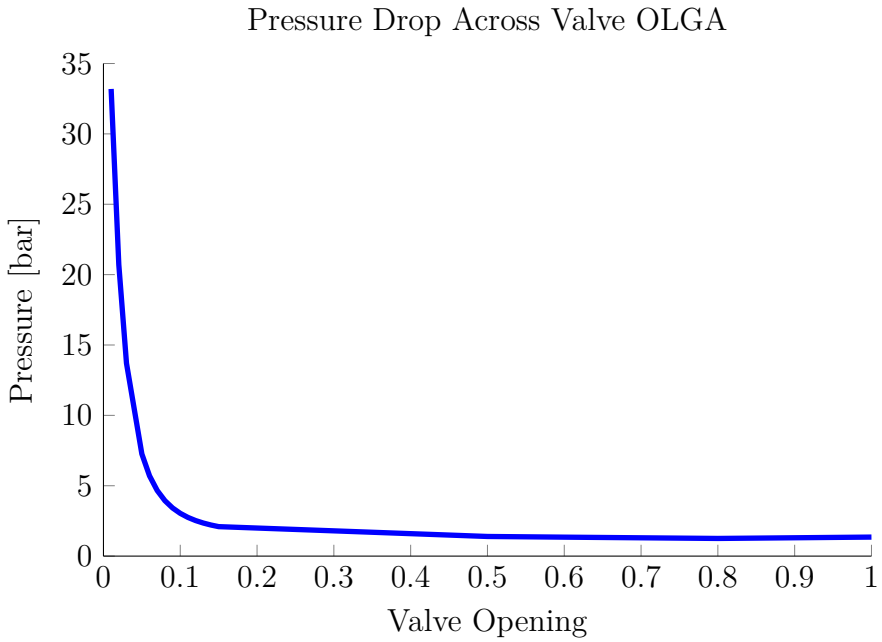

Figure 22: Pressure drop across the valve as a function of valve opening. The data is obtained from OLGA.

Valve Equation Approach

By using the valve function obtained in section 8.2.1:

$$f(z) = 0.13(1 - \exp(-9z))$$

and combining it with Equation 40, we obtain a pressure drop estimation as presented in Figure 23.

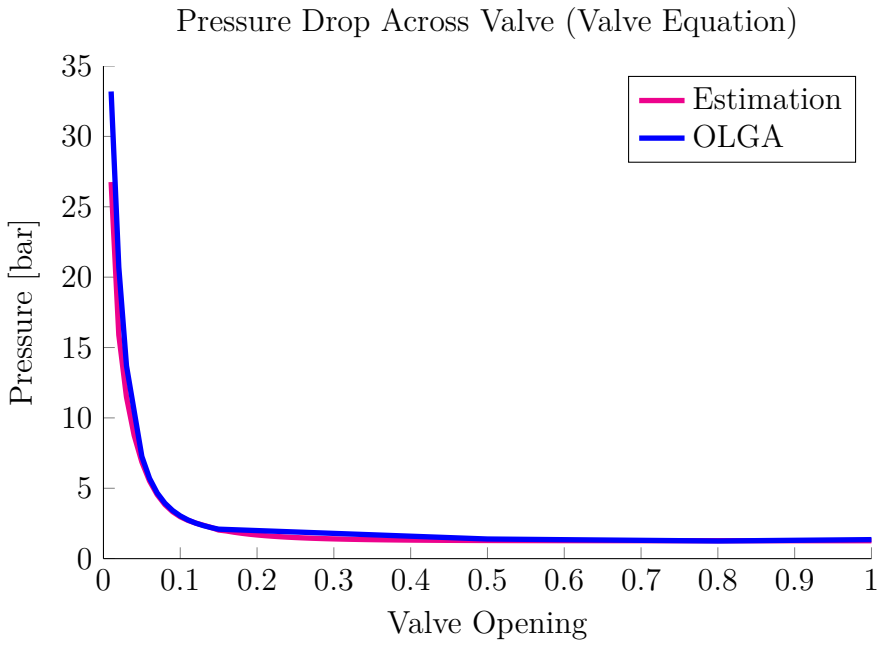

Figure 23: A comparison of the pressure drop estimated with the valve equation, and the actual pressure drop across the valve.

Figure 23 shows a comparison of the estimation and the pressure drop profile from OLGA. We see that the this method gives a very good estimation of the pressure drop across the valve. The areas in Figure 23 with the largest deviations between estimation and OLGA profile, is also the area where the valve equation is poorest fitted. This can be seen in Figure 21.

Bernoulli Approach

The pressure drop is estimated from Equation 29, which is derived in chapter 8.1. The result, presented in Figure 24, shows that the estimate by the Bernoulli Approach flattens out at a lower value than the pressure drop values generated in OLGA. For valve openings between 0.1 and 1.0 the pressure drop decreases from 0.99 bar to 0.0032 bar, which is slightly lower than for the real values. Apart from that, the trend is very similar. Also here, the pressure drop across the valve only gets large for very small valve openings.

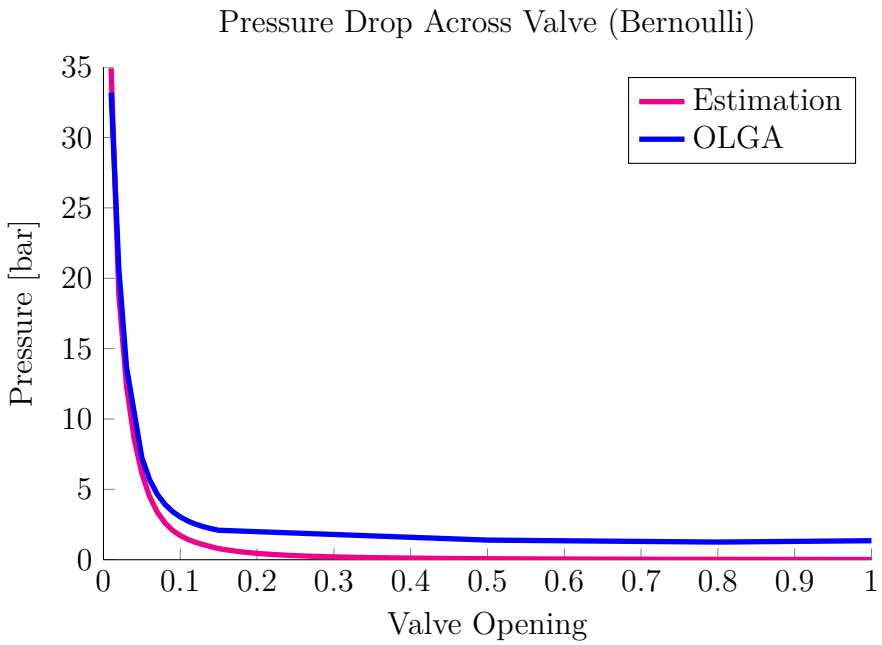

Figure 24: A comparison of the pressure drop estimated by the Bernoulli approach, and the actual pressure drop across the valve.

One reason for the deviation between OLGA and the estimate, can be that the estimation is based on a more ideal model than what is realistic. In a real case there may occur more energy loss than what is accounted for in our model, which again would result in a larger pressure drop.

In our valve-model, the C_d-factor is the only factor which accounts for deviation between a theoretical and a real case. For the estimate presented in Figure 24, this factor is set to 0.84, which is the same value as for the C_d-factor in OLGA. However, it is likely that deviations from the theoretical case in OLGA are corrected for in other places than only in the C_d-factor. It looks like the valve in OLGA has a minimum pressure drop of approximately 1.3$[bar]$. This is reasonable, as there in a real case always will be some friction loss, also at valve opening 1.

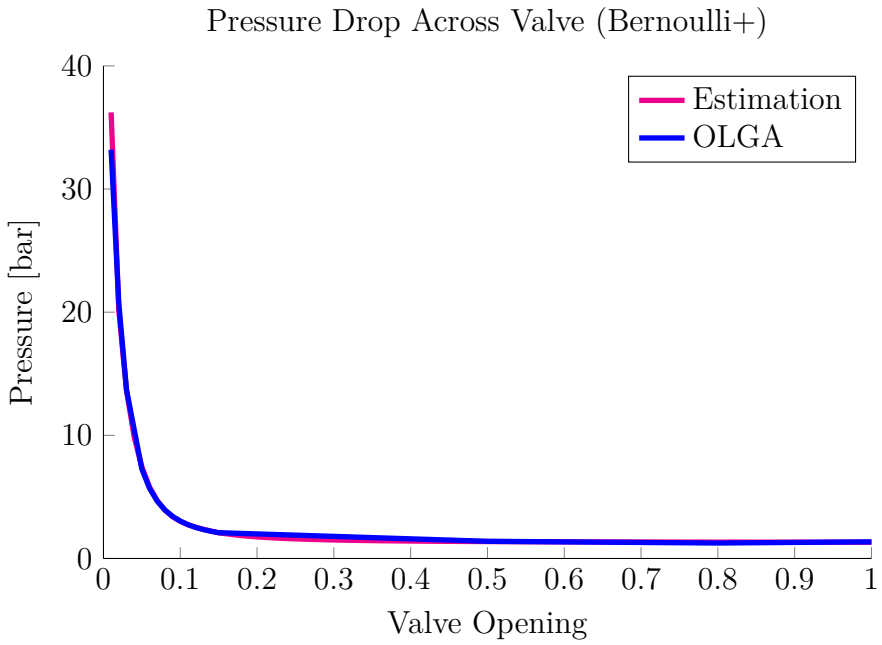

Figure 25: A comparison of the pressure drop estimated by Equation 42, and the actual pressure drop across the valve.

$$\triangle p = \rho \left(\frac{q}{C_d f(z) A} \right)^2 + \triangle p_{min} \tag{42}$$

By adding a minimum pressure drop value to Equation 40 ($\triangle p_{min} = 1.3[bar]$),

we obtain the pressure drop estimation presented in Figure 25. We see from the estimation
adding friction-loss or a

8.2.3 Comparing the Valve Equation- and Bernoulli Approach

Both the Bernoulli approach(+ constant pressure drop factor) and the Valve Equation approach give good estimations for the pressure drop across the valve in our system.

An assumption that must be met for Bernoulli's equation to apply, is that friction forces must be negligible. This is not the case in most valves used in process facilities. Some of the energy loss is accounted for by including the C_f-factor, and the remaining in the *minimum pressure drop*($\triangle p_{min}$). The pressure drop estimated by this method will highly depend on these two factors, and therefore be much more empirical than it appears to be, being based on Bernoulli.

By identifying the flow characteristics and an empirical valve equation, we obtained a very good estimation for the pressure drop.

9 Further Work

If the model presented in this thesis should be used for other purposes than obtaining information on trends and approximate pressure-values as a function of valve opening, several improvements should be made.
The model developed in this thesis is dependent on a polynomial function that calculates the flow as a function of valve opening. This function has been made from data obtained in OLGA, and the MATLAB-model is therefore not completely independent of the OLGA model. An improvement would be to eliminate this dependence.

A suggestion is to start modelling from the valve and down. Here we can often measure the initial value for the pressure, which gives enough information for the integration. In this thesis the modelling was started from the bottom of the well and up. Here we had no initial conditions available, and the flow therefore was estimated by simulation-data.

10 Conclusion

In this thesis a simple MATLAB-model is made based on basic physical principles. The quality of the model is evaluated by making a similar model in OLGA, and comparing the results from the MATLAB-model with data obtained from the OLGA-simulations.

The model is combined of three flow models; inflow-, pipeflow-, and a valve model. In the finished model these three parts are linked together, and made a function of the valve opening. The principles used for the inflow-, pipeflow-, and valve model is respectively Darcy's law, the Compressibility EOS and the Valve Equation. By comparing the results from the MATLAB-model with the results from the OLGA-simulations, we see that the principles give a good approximation of the pressure relations in the well.

The model works best for the or the purpose of obtaining information on trends and approximate pressure-values at different as a function of valve opening. However, this is a *very* simplified model, which is also partly adapted to dataseries obtained from OLGA, and should therefore be improved at several areas and tested before used for other purposes.

11 References

Buckley, S. Page.(1964). Techniques of Process Control. John Wiley & sons.

Foss, B. (2012).Process control in conventional oil and gas fields - Challenges and opportunities. Control Engineering Practice, 20, 1058-1064.

Gunnerud,V.,Foss,B.(2009). Oil production optimization âĂŞ A piecewise linear model, solved with two decomposition strategies. *Computers and Chemical Engineering*, 34(11),1803-1812.

Hubbert, M. King.(1956). Darcy's law and the field equations of the flow of underground fluids.*Journal of Petroleum Technology*.

Jansen,J. D., Bosgra, O. H., & van den Hof, P. M. J.(2008). Model-based control of multiphase flow in subsurface oil reservoirs. *Journal of Process Control*, 18(9),846-855.

McCain, W. D.(1990). The Properties of Petroleum Fluids, 2. ed. Penwell Books.

Skogestad, S.(2000). Plantwide control: The search for the self-optimizing control structure. *Journal of Process Control*, 10, 487-507.

Skogestad, S.(2009). Chemical and Energy Process Engineering. Taylor & Francis Group: CRC Press.

Standing, M. B., Katz, D. L.(1942). Density of natural gases. Trans, AIME, 146, 144.

Appendices

A Well Performance Curves

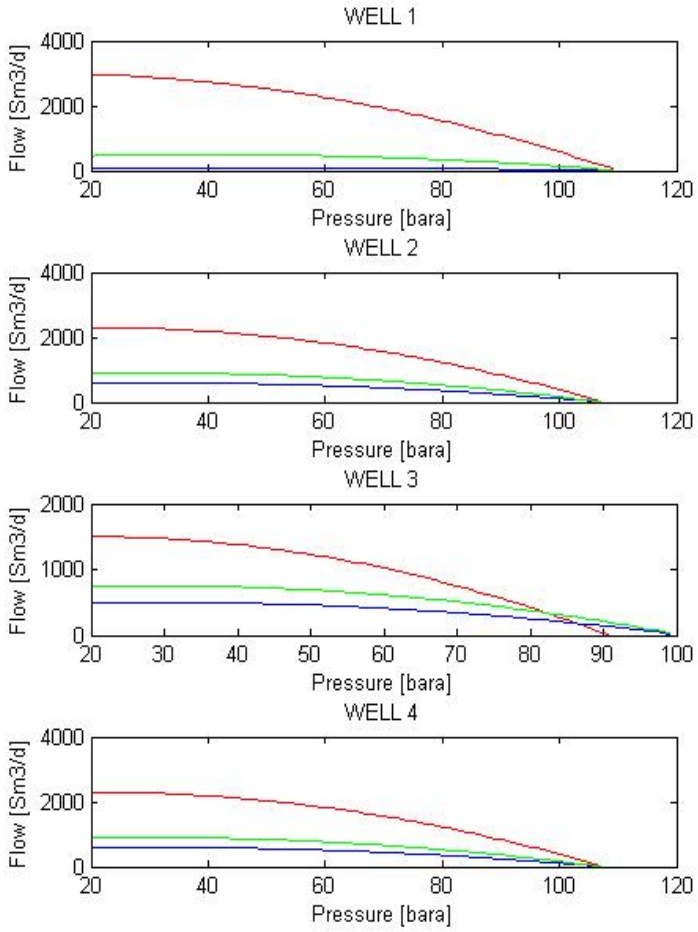

Figure 26: Well Preformance Curves from the Troll-dataset.

B Valve specifications

Table 4: Valve Specifications in Olga

	Model	Equilibrium model	Slip model	Thermal Phase
Valve 1(-4)	Hydrovalve	Frozen	No Slip	No

Hydromodel - used for chokes and valves with liquid/gas characteristics.

Frozen is the equilibriummodel for no mass transfer.

No Slip is assumed in our valve model.

No thermal phase means that the gas will expand isentropical while the liquid is isotermal.

C Relevant Data From OLGA-simulations

Data for the four wells, obtained from simulations in OLGA*

*flowpath 3 is not included at iit has the exact same properties as flowpath 1.

Gas, oil and water flows are give in [m^3/day], pressure is given in [bar] and, temperature is given in [^oC].

flowpath 1

Valve	gas	oil	water	pressure	temp
1	523,793	178,504	292,11	53,3568	60,6744
0,5	522,75	178,345	291,84	53,4043	60,6746
0,15	506,119	175,764	287,472	54,1762	60,6781
0,14	503,46	175,344	286,762	54,3018	60,6786
0,1	484,74	172,321	281,652	55,2089	60,6826
0,09	476,422	170,942	279,322	55,6238	60,6844
0,08	465,445	169,086	276,189	56,1828	60,6868
0,07	450,685	166,523	271,866	56,9563	60,6902
0,06	430,268	162,87	265,712	58,0607	60,6948
0,05	402,087	157,49	256,662	59,6944	60,7016
0,03	361,942	149,247	242,831	62,2099	60,7118
0,02	304,989	136,112	220,874	66,2688	60,7271
0,01	225,448	113,988	184,145	73,162	60,7519

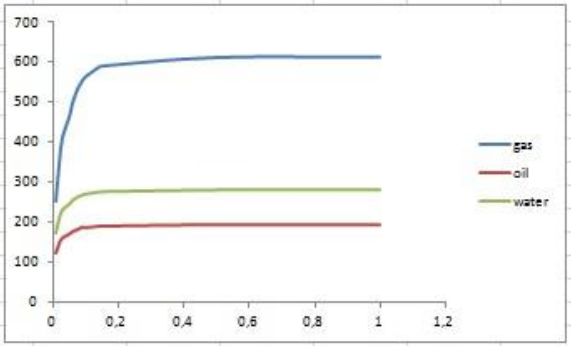

flowpath 2

Valve	gas	oil	water	pressure	temp
1	613,746	193,709	281,898	52,9264	57,6276
0,5	612,401	193,522	281,616	52,979	57,698
0,15	591,064	190,5	277,066	53,8303	57,7035
0,14	587,678	190,01	276,329	53,9684	57,5044
0,1	563,912	186,493	271,038	54,9622	57,7082
0,09	553,431	187,894	268,636	55,4146	57,7098
0,08	539,672	182,752	265,416	56,0222	57,7119
0,07	521,29	179,804	260,994	56,8596	57,7148
0,06	496,268	175,625	254,731	58,0484	57,7189
0,05	461,692	169,514	245,587	59,7935	57,7247
0,03	413,4114	160,24	231,749	62,4536	57,7335
0,02	346,149	145,62	210,024	66,6851	57,7466
0,01	253,727	121,265	174,087	73,8011	57,7674

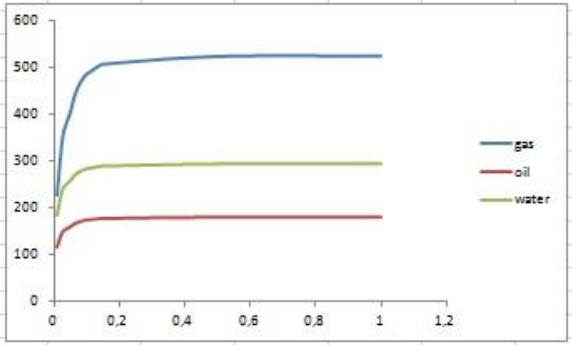

flowpath 4

Valve	gas	oil	water	pressure	temp
1	635,242	205,628	263,427	52,4184	52,9577
0,5	633,342	205,363	267,076	52,4901	52,9581
0,15	609,314	201,949	258,547	53,4172	52,9633
0,14	605,664	201,417	257,843	53,5615	52,9641
0,1	580,432	197,657	252,861	54,5854	52,9698
0,09	569,436	195,966	250,623	55,0466	52,9723
0,08	555,079	193,709	247,637	55,6632	52,9757
0,07	535,999	190,618	243,553	56,509	52,9803
0,06	510,158	186,255	237,794	57,7049	52,9867
0,05	474,603	179,892	229,409	59,4546	52,9958
0,03	425,115	170,249	216,739	62,1157	53,0094
0,02	356,175	155,011	196,798	66,3502	53,0233
0,01